Food Hydrocolloids 138 (2023) 108486

Contents lists available at ScienceDirect

Food Hydrocolloids

journal homepage: www.elsevier.com/locate/foodhyd

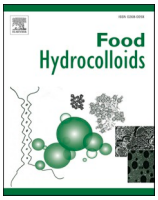

Adsorption kinetics and dilatational rheology of plant protein concentrates at the air- and oil-water interfaces

Vassilis Kontogiorgos *, Sangeeta Prakash

School of Agriculture and Food Sciences, The University of Queensland, Brisbane, 4072, QLD, Australia

ARTICLE INFO

Keywords:
Plant protein
Lissajous
Dilatational
Rheology
Terpene
Kinetics

ABSTRACT

Adsorption kinetics and dilatational rheology of plant protein concentrates at the air- and oil-water interfaces were investigated at pH 7.0 in 100 mM NaCl. Three interfaces (air-water, triglyceride-water and terpene-water) and four protein concentrates (soy, pea, mung bean and rice) were examined. The dynamic interfacial properties were monitored by axisymmetric drop shape analysis. Kinetic modelling of the early and advanced stages of protein adsorption was carried out using the Ward-Tordai and Graham-Philips thermodynamic approaches. Construction of surface pressure master curves revealed a pseudo equilibrium plateau for legume proteins of ~20, 12, and 22 mN/m at the air, triglyceride and terpene interfaces, respectively. In contrast, rice proteins have a lower capacity to increase the surface pressure at the oil interfaces (<15 mN/m). Data modelling revealed that diffusion is mostly independent of the protein composition, but protein rearrangement at the interfaces was faster at the oil than at the air interfaces. Dilatational rheological measurements revealed more elastic films at the air than at oil interfaces, with the dilatational storage modulus reaching values up to 37 mN/m. The least elastic films were formed at the terpene interfaces, with storage moduli being <25 mN/m for all isolates investigated. Lissajous plot construction revealed a strain-hardening behaviour of films upon compression and strain-softening on extension, the magnitude of which follows the order air > terpene > triglyceride. Overall, results show that botanical source and subphase composition are critical in selecting the optimum stabilisation strategy in multiphasic foods using plant proteins.

1. Introduction

Research on plant proteins has gathered pace in the last decade as a response to rapid cultural changes and exploration of sustainable protein sources (Aiking & de Boer, 2020; Loveday, 2019). Proteins are essential components in structuring multiphasic foods because of their broad range of functionality, including interfacial adsorption. Proteins from animal sources, especially those from the dairy or egg industries (e.g., whey or egg white proteins), are the main proteins used as functional ingredients in food formulation. Although plant proteins may also be used, they have an inferior technological performance compared to those from animal sources and fail to replace them efficiently. In the formulation of dispersed systems, in particular, the main reason lies behind the viscoelasticity of the interfacial film. Animal-based proteins form stiffer viscoelastic films after adsorption at interfaces. In contrast, the plant-based protein layers are significantly weaker primarily due to their compact 3D structure and low aqueous solubility (Sagis & Yang, 2022).

Despite these drawbacks, research to better understand the interfacial properties of plant proteins to improve their functionality continues unabated (Drusch, Klost, & Kieserling, 2021). While the interfacial rheology of animal proteins (e.g., β-caseins or bovine serum albumin) is a well-established field, research on the behaviour of plant proteins at interfaces is scattered in the literature. For example, proteins from plant sources have been shown to exhibit excellent interfacial characteristics, and their botanical source and subphase composition are of foremost importance for their functionality (Ducel, Richard, Popineau, & Boury, 2004; Mileti et al., 2022; Romero et al., 2012; Wang et al., 2012; Wojciechowski, 2022). Theoretical treatment of adsorption kinetics has been first explored by Ward and Tordai (Ward & Tordai, 1946). This treatment considers adsorption as a diffusion-controlled process, assuming that the surfactant diffuses from the bulk into the subsurface. Once at the subsurface, it directly adsorbs at the interface. They arrived at the classic equation:

* Corresponding author.
E-mail address: v.kontogiorgos@uq.edu.au (V. Kontogiorgos).

https://doi.org/10.1016/j.foodhyd.2023.108486
Received 17 October 2022; Received in revised form 4 January 2023; Accepted 13 January 2023
Available online 16 January 2023

$$\Gamma(t) = 2c_o\sqrt{\frac{Dt}{\pi}} - 2\sqrt{\frac{D}{\pi}}\int_0^{\sqrt{t}} c_s d(\sqrt{t-\tau}) \quad (1)$$

where c_o is the bulk surfactant concentration, D is the diffusion coefficient, c_s is the concentration in the subsurface, π is 3.14, and τ is a dummy variable of integration (Eastoe & Dalton, 2000). The first term accounts for the initial stage of the adsorption process, and the second for the back diffusion of the surfactant. At short times where $t \rightarrow 0$ and the surface pressure is < 1 mN/m, there is no back diffusion, and the second term can be neglected (i.e., dilute solutions). Consequently, by using the first term is possible to model the adsorption kinetics of dilute protein solutions at the air-water or oil-water interfaces. At higher concentrations, however, where an energy barrier to interfacial adsorption exists, protein diffusion is no longer the determining factor for its adsorption. Instead, protein penetration and rearrangement at the interface are now the two rate-limiting steps. It is possible to monitor the kinetics of these two events with a first-order kinetic approach using the equation (Graham & Phillips, 1979a):

$$ln\frac{\pi_f - \pi_t}{\pi_f - \pi_o} = -kt \quad (2)$$

where π_f and π_o are the final and initial surface pressures, π_t is the surface pressure at time t, and k is a first-order rate constant.

However, the fragmented nature of the work makes it difficult to assess and compare the functionality of plant protein concentrates at different interfaces. The present study attempts to bridge this gap by studying a number of industrially significant plant protein concentrates and exploring their behaviour at various interfaces. The current work aims to facilitate the creation of multiphasic foods using plant proteins, and its objectives are to explore the adsorption kinetics of plant protein concentrates and the rheology of their interfacial films at subphases with different chemical compositions.

2. Materials and methods

2.1. Materials

Pea protein isolate (PP) was purchased from Pure Product Australia (Mascot, NSW), soy (SP) and rice (RP) from Bulk Nutrients (Grove, TAS) and mung bean (MBP) from Australian Plant Proteins (Horsham, VIC). Trizma base, NaCl, bentonite, and myrcene were obtained from Sigma-Aldrich (St Louis, MO). Medium-chain triglyceride oil (MCT) MIGLYOL 812 N was purchased from IOI Oleochemical (Witten, Germany). Milli-Q water was used throughout the experimental work.

2.2. Sample preparation and characterisation

Protein concentrates were dispersed at a nominal concentration (amount of protein powder dispersed in buffer) of 1 mg/mL in a 100 mM Tris buffer at pH 7.0 with 100 mM NaCl to form a stock solution. The stock solution was left stirring for 10 min at room temperature before being centrifuged at 23000×g for 15 min. Following centrifugation, two serial dilutions with the buffer (10 and 100 times) of the stock solution resulted in two additional samples with nominal protein concentrations of 0.1 mg/mL and 0.01 mg/mL. The actual concentrations of the samples are shown in Table 1. For simplicity, samples are labelled as 1, 0.1 and 0.01 mg/mL throughout. Prior to measurements, solutions were filtered with a 0.45 μm disk filter (Millex-HA, Millipore). Before filtration, the cartridge was washed with 10 mL of buffer and 5 mL of the protein solution. After washing, 15 mL of the protein solutions were filtered and kept for interfacial studies. Bentonite was dispersed in myrcene at 15% w/v and left under magnetic stirring for 2 h at room temperature. The dispersion was centrifuged for 20 min at 5000×g to remove bentonite, and the supernatant was used for interfacial studies. Bentonite clarification is essential as it removes surface active components that are present in myrcene after manufacturing that interfere with surface tension measurements.

2.3. Electrophoresis and sample characterisation

Electrophoresis was conducted under reducing conditions (β-mercaptoethanol) using the Bio-Rad Mini Protean Tetra Cell System on a 4–20% Mini-PROTEAN TGX Precast Protein Gels at 100 V for 1 h (Bio-Rad Laboratories, Inc., US) and stained with Coomassie Blue stain. The protein content of the stock solutions prepared for interfacial measurements was determined using the Bradford assay (Bradford, 1976) with bovine serum albumin as standard to construct the calibration curve. The protein, lipid and carbohydrate contents of protein concentrates are reported by the manufacturers and shown in Table 1.

2.4. Dynamic interfacial tension measurements

A glass Hamilton syringe (DS500/GT) equipped with a stainless-steel dosing needle with a 1.6 mm outer diameter (SNP 160/119) was used in the experimental setup. The syringe was washed with 2 mL of buffer and 1 mL of filtered protein solution before loading it for measurements. Surface tension measurements using only buffer were performed regularly to ascertain the absence of surface-active contaminants in the needle. The density of the oils used in the measurements were 0.945 and 0.791 g/mL for MCT and myrcene, respectively, while that of the buffer was taken as 0.997 g/mL. Dynamic interfacial tensions of the samples were monitored using axisymmetric drop shape analysis with a pendant drop tensiometer (OCA-15EC, DataPhysics Instruments, Germany) using the Young-Laplace fitting. A drop with an area of ~30 mm^2 was formed, and the evolution of the surface pressure ($\pi = \gamma_o - \gamma_t$) with time was monitored for 30 min, where γ_o is the interfacial tension of buffer and γ_t is the interfacial tension of the protein sample at time t. All measurements were performed in duplicates, and average values are reported.

2.5. Dilatational rheology

Only solutions with a nominal protein concentration of 1 mg/mL were taken forward for dilatational rheological measurements. A drop with an approximate surface area of ~25 mm^2 was formed for the experiments at the air surfaces and left to rest for 15 min to dissipate loading stress. A drop of ~15 mm^2 was formed for the MCT and myrcene interfaces, followed by the same resting phase. Following the resting period, strain sweeps were performed at a frequency of 0.1 Hz with a

Table 1
Composition of protein concentrates reported by the manufacturers (protein, lipids, carbohydrates). The actual protein concentration of stock solutions with a nominal concentration of 1 mg/mL was measured with the Bradford assay. Values with the same letter are not significantly different at $p > 0.05$. Protein solutions with a nominal concentration of 0.1 mg/mL and 0.01 mg/L were produced with serial dilutions of the 1 mg/mL stock solution.

Sample	Protein (% w/w)	Lipids (% w/w)	Carbohydrates (% w/w)	1 mg/mL stock solutions (x10^{-3} mg/mL)	0.1 mg/mL solutions (x10^{-3} mg/mL)	0.01 mg/mL solutions (x10^{-3} mg/mL)
PP	86	6.5	5	28 ±2^a	2.8	0.28
SP	88	1.5	0.5	40 ±3^a	4	0.4
MBP	88	6	3	33 ± 10^a	3.3	0.33
RP	81	2	6	13 ±2^b	1.3	0.13

strain amplitude varying between 10 and 50%. Mechanical spectra were obtained by employing a sinusoidal perturbation with deformation amplitudes $\Delta A/A_o$ of ~10% within the linear viscoelastic range (LVR) of the interfaces and frequencies between 0.01 and 1 Hz. All experiments were performed at room temperature. Lissajous plots were constructed by plotting the π vs $(A-A_o)/A_o$, where A_o is the area at zero deformation. All measurements were performed in duplicates, and average values are reported.

3. Results and discussion

3.1. Sample characterisation

All protein isolates used in the present work had more than 80% w/w protein and contained variable amounts of lipids and carbohydrates co-extracted during the isolation process (Table 1). Carbohydrates in protein concentrates are usually starch granules and insoluble cellulosics that remain after protein extraction. These insoluble compounds were removed during the centrifugation and filtration steps. Any remaining monosaccharides (e.g., glucose) do not have interfacial activity. The formation of Maillard conjugates during protein extraction could be a source of interfacial activity (Li, McClements, Liu, & Liu, 2020) and cannot be ruled out. However, their concentration should have a negligible contribution to the overall surface activity of the isolates. In contrast, lipids (e.g., mono- and diacylglycerols or phospholipids) may influence the functional properties of protein isolates even when they are present in small amounts (Ma et al., 2022). Usually, these lipids are not associated with the proteins, but they originate from the isolation process through cell and organelle rupture, largely depending on the isolation processes (e.g., wet vs dry extraction) (Ma et al., 2022; Sim, Srv, Chiang, & Henry, 2021). It should be stressed that it is impossible to quantitatively separate lipids in any meaningful manner, and any remaining should always be regarded as an integral part of the samples.

Proteins were dispersed at a nominal concentration of 1 mg/mL at pH 7.0 in the presence of salt yielding actual protein concentrations shown in Table 1 corresponding to a protein solubility of ~30–40% for PP, SP and MBP and ~13% for RP. Plant protein solubility depends on many factors, including solution pH, solubilisation time or temperature, just to name a few. RP had significantly different solubility from the rest, which may cause difficulties directly comparing the samples, but it permits first insights into their interfacial behaviour.

Plant proteins primarily consist of globulins and albumins in a ratio of approximately 60:20, depending on the cultivar and other agronomical characteristics (Day, 2013). Electrophoresis identified all major proteins in the samples in accordance with previously published work (Fig. 1) (Djoullah, Djemaoune, Husson, & Saurel, 2015; Mendoza, Adachi, Bernardo, & Utsumi, 2001; Nishinari, Fang, Guo, & Phillips, 2014; Van Der Borght et al., 2006). PP, SP, and MBP proteins are generally readily soluble at neutral pH containing salt, while RP isolates, consisting of prolamins and glutelins, have limited solubility because of the very low content of charged amino acids.

3.2. Adsorption kinetics

Transient surface pressures were monitored for 30 min at the air- and oil-water interfaces for all systems at three nominal protein concentrations (0.01, 0.1, and 1 mg/mL) and plotted as a function of time (Fig. 2a). All systems exhibited qualitatively a similar behaviour irrespectively of protein concentration and interface. The surface pressure increases exponentially at the initial stages of adsorption and reaches a pseudo-equilibrium plateau at longer times. It is possible to extend the observational time by constructing surface pressure master curves with the application of an empirical time-concentration superposition of the data (Poirier et al., 2021). The reference concentration to shift the experimental data along the x-axis was chosen as 0.1 mg/mL (Fig. 2b–d). When plotted as a function of the normalised time αt with the shift factor

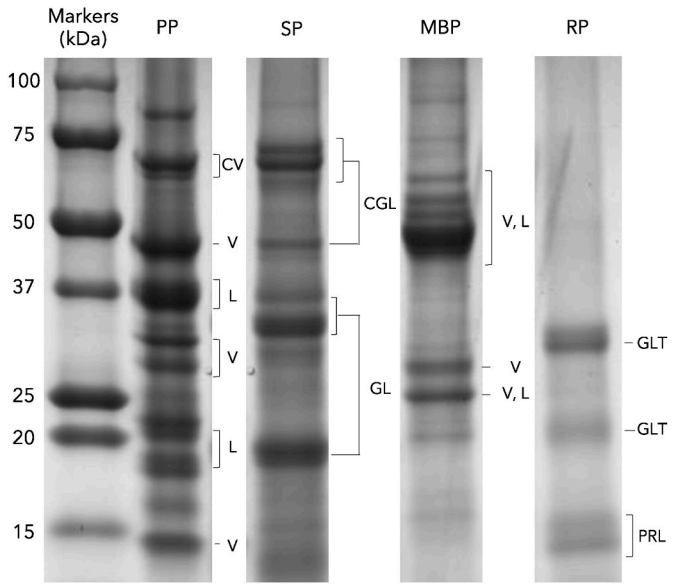

Fig. 1. Electrophoretic patterns of protein concentrates. CV: convicilin, V: vicilin, L: legumin, CGL: conglycinin, GL: glycinin, GLT: glutelin, PRL: prolamin, PP: pea protein, SP: soy protein, MBP: mung bean protein and RP: rice protein.

$\alpha = t/t_r$, data fall into a single master curve (t is the time and t_r the time at the reference concentration). All master curves reveal three distinct features. In the first regime, an induction period can be observed for all systems with infinitesimal changes in the surface pressure (Fig. 2b). In this regime, although protein may be at the interface, it has a limited capacity to depress the surface tension of the systems. Remarkably, the end of the induction period is between 10 and 100 s regardless of the interface and protein, suggesting that the diffusion kinetics in the aqueous phase is the controlling event in this regime. The induction period observed is in the same order as those observed for other plant protein concentrates (Mileti et al., 2022). A steep increase follows at the end of the induction period in the surface pressure. In this regime, proteins sufficiently cover the interface and depress the surface tension. In protein systems, it is the first adsorbed layer that mostly influences π, whereas, at higher concentrations, adsorption continues with an increase in the film thickness and minor changes in π (Graham & Phillips, 1979b). Finally, in the last regime, a pseudo-equilibrium plateau is reached. It should be mentioned that a true equilibrium in protein systems is usually not established as rearrangements at the interface, and ageing of the interfacial film is a continuous process (Beverung, Radke, & Blanch, 1999; Bos & van Vliet, 2001). A departure from a satisfactory data shifting in the last regime indicates other factors influence the formation of interfacial protein layers, including chain interactions and ageing. However, the plateau values for the legume proteins converge irrespective of the interface, indicating that the structural differences between the proteins are not a distinguishing characteristic of their interfacial behaviour.

At the air-water interfaces, soy proteins showed a pseudo plateau surface pressure of ~18 mN/m, a value very close to ~19 mN/m under similar conditions (pH 7.0, 1 mg/mL) (Xia, Botma, Sagis, & Yang, 2022). At the triglyceride interfaces, soy proteins resulted in a π of ~12 mN/m, a value indistinguishable from those obtained for corn oil interfaces (Wang et al., 2012). Consistent with our findings, previously published investigations on vicilins from various sources (e.g., pea, kidney and mung beans) have also been reported to create a π of ~12 mN/m at triglyceride-water interfaces (Chang, Tu, Ghosh, & Nickerson, 2015; Liang & Tang, 2013; Liu, Chen, & Tang, 2014; Shen & Tang, 2014). Rice proteins did not establish equilibrium, and at the air interfaces, they exhibited higher surface pressures (Fig. 2b). A similar trend has been

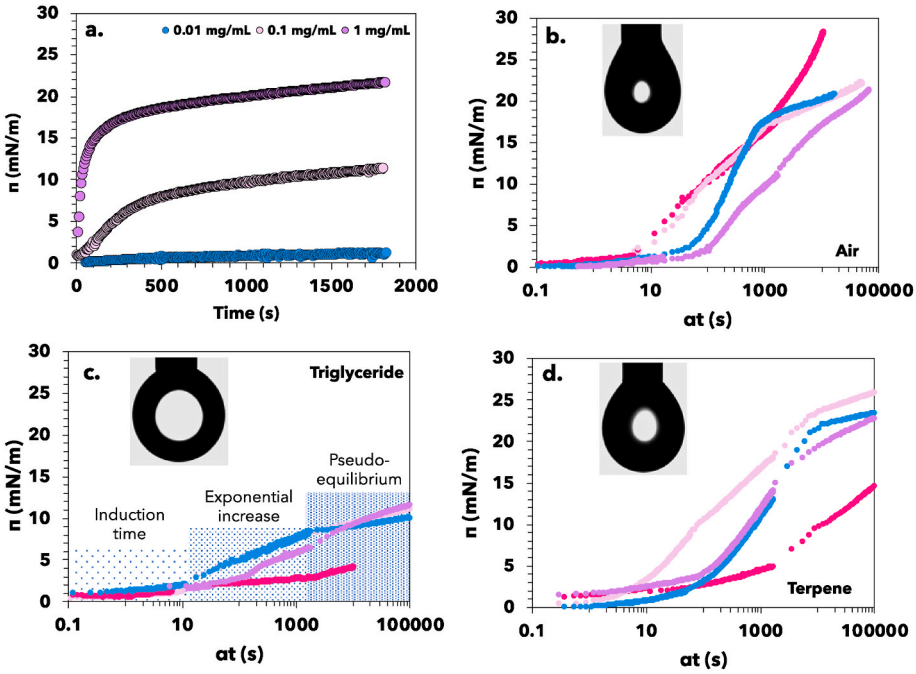

Fig. 2. a) Typical surface pressure isotherms of plant protein isolates at three different concentrations (curves for MBP at the air interface). Superposition of data in (a) as a function of normalised time (αt) results in surface pressure master curves at b) the air-water, c) triglyceride-water, and d) terpene-water interfaces. The insets show a macroscopic image of the pendant drop at different interfaces. PP (●), SP (○), RP (●) and MBP (●).

previously observed at air-water interfaces for rice protein compared with those from soy and hemp, and it has been proposed that this is due to their lower molecular weight making them able to diffuse faster at the interface (Mileti et al., 2022). Wheat gluten hydrolysates that have structural similarities with rice proteins showed an estimated pseudo equilibrium surface tension at the air-water interfaces of ~47 mN/m (Wouters et al., 2017), which is in the same range as the values obtained for rice proteins from the present investigation (~45 mN/m). It should be noted, however, that while rice proteins showed much higher surface activity at the air interface, they had the least capacity to increase the surface pressure at oil-water interfaces (Fig. 2 c, d). Surface pressure values at the end of the measurements were around 5 and 18 mN/m for the triglyceride and terpene interfaces, respectively. A molecular weight dependency for rice glutelin has been found at the corn oil interfaces (i.e., triglyceride) at pH 7.0 with low molecular weight glutelins resulting in surface pressures of ~10 mN/m (Yang, Dai, Sun, McClements, & Xu, 2022). In the present investigation, the rice proteins resulted in a π of ~5 mN/m, a similar trend despite the differences between the two systems. This indicates that glutelins play a decisive role in the diffusion kinetics of rice protein concentrates to triglyceride interfaces, although the presence of prolamins cannot be disregarded. It starts emerging that the botanical family (i.e., Poaceae vs Fabaceae) may be a distinguishing characteristic for plant protein functionality.

Similar trends were also observed for the terpene interfaces. However, the pseudo plateau surface pressures created for all systems were higher (~22 mN/m) than those of triglyceride interfaces and comparable to those of air interfaces (Fig. 2d). These findings are consistent with the behaviour of proteins at limonene interfaces, although the surface pressure values were substantially higher at the air-water surface than at the limonene-water interface (Mitropoulos, Mütze, & Fischer, 2014). MCT oil is a medium polarity oil due to oxygen and medium-length fatty acids (caprylic C8:0 and capric C10:0) in contrast with the apolar hydrocarbon chain of myrcene. It has been shown that as the polarity of the subphase increases, the surface pressures generated by protein adsorption decrease (Bergfreund, Bertsch, & Fischer, 2021; Bergfreund, Bertsch, Kuster, & Fischer, 2018). Our data were consistent with this generalisation as samples in the MCT subphases showed lower surface pressures than in myrcene and air. These initial observations show that the solubility of protein concentrates in the subphase is critical for their interfacial performance.

Protein adsorption kinetics involves three events: the transit of protein from the bulk to the subsurface because of a concentration gradient, the adsorption of protein from the subphase to the interface and, once at the interface, the conformational rearrangements and interactions that dictate the properties of the interfacial film (Beverung et al., 1999). To pinpoint any differences in the kinetics of the adsorption of protein concentrates, we proceeded with quantifying these events using equation (1). Accordingly, when protein arrival at the subphase is a diffusion-controlled process, the slope of the π vs $t^{1/2}$ curves yields a diffusion rate constant (k_{diff}) (Fig. 3a) that can be used to compare the diffusion rates of proteins (Table 2). Inspection of the table reveals no appreciable differences in the diffusion rates to the air surface between protein isolates. Consequently, the diffusion is not responsive to protein isolate composition regardless of their molecular complexity (Fig. 1) and compositional discrepancies (Table 1). All proteins diffuse faster towards the terpene and somewhat slower towards the triglyceride interfaces than air. Hydrophobic amino acids may have a greater affinity for the myrcene that facilitates the transfer of proteins from the bulk to the interface.

For the samples at higher concentrations (1 mg/mL), where an energy barrier to interfacial adsorption exists, we used equation (2) to model the adsorption kinetics. Curves of $\ln((\pi_f - \pi_t)/(\pi_f - \pi_o))$ vs t are characterised by two dominant features representing the two kinetic processes (Fig. 3b). The first slope yields the adsorption rate constant (k_{ads}), whereas the second is the interfacial rearrangement rate constant (k_{rear}). Calculating all slopes (Table 2) reveals modest differences between k_{ads} of the proteins in all samples, with the terpene interfaces somewhat facilitating interfacial adsorption. However, a striking difference was observed in the k_{rear} constant. At the triglyceride interfaces, the rearrangement was twice as fast as those in the air, whereas it was almost three times faster in the myrcene showing that proteins unfold and rearrange at the oil interfaces faster than at the air surfaces.

Our analysis yields comparable (Liu et al., 2014; Wang et al., 2012), lower (Mileti et al., 2022; Shen et al., 2014; Yang, Dai, et al., 2022) or

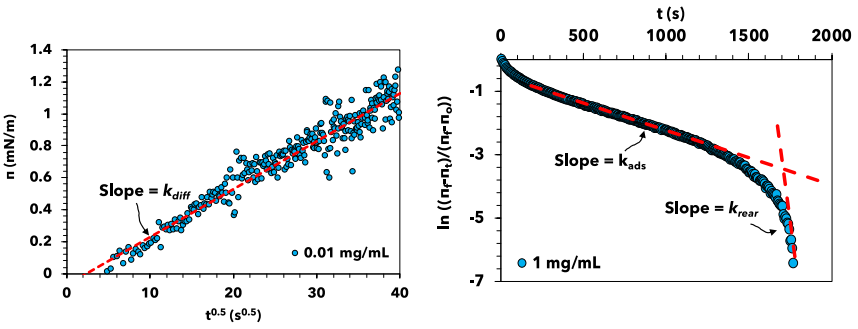

Fig. 3. a) Typical kinetic plot at a nominal concentration of 0.01 mg/mL. The slope of this curve is the k_{diff}, b) Typical kinetic plot at a nominal concentration of 1 mg/mL. The first slope yields the adsorption (k_{ads}), and the second the rearrangement (k_{rear}) rate constants.

Table 2
Diffusion (k_{diff}), adsorption (k_{ads}) and rearrangement (k_{rear}) rate constants for all samples and interfaces. AIR: air, MCT: triglyceride, MYR: terpene. k_{diff} rate constants have been obtained for samples with 0.01 mg/mL protein concentration using the Ward-Tordai data treatment. k_{ads} and k_{rear} rate constants have been obtained for samples with 1 mg/mL protein concentration using the Graham-Philips data treatment. The minus sign indicates negative slopes, and the number in the parenthesis is the linear regression coefficient of each sample.

	k_{diff} x10^{-3} (mN/m s$^{-0.5}$)			-k_{ads} x10^{-3} (s^{-1})			-k_{rear} x10^{-3} (s^{-1})		
	AIR	MCT	MYR	AIR	MCT	MYR	AIR	MCT	MYR
PP	31 ± 2.8 (0.933)	28 ± 7.1 (0.929)	51 ± 8.4 (0.993)	1.5 ± 0.2 (0.982)	1.8 ± 0.2 (0.986)	2.1 ± 0.4 (0.992)	7.2 ± 1.1 (0.685)	12 ± 2.8 (0.862)	21 ± 4.2 (0.605)
RP	33 ± 5.7 (0.855)	24 ± 5.6 (0.838)	74 ± 7.1 (0.995)	1.3 ± 0.2 (0.986)	1.8 ± 0.2 (0.975)	1.9 ± 0.5 (0.998)	7.3 ± 1.2 (0.881)	13 ± 0.7 (0.629)	20 ± 2.8 (0.746)
SP	35 ± 4.2 (0.983)	26 ± 4.3 (0.960)	52 ± 9.9 (0.994)	1.4 ± 0.7 (0.985)	1.7 ± 0.4 (0.988)	2.0 ± 0.1 (0.996)	8.3 ± 0.7 (0.852)	14 ± 1.4 (0.648)	28 ± 1.4 (0.921)
MBP	32 ± 2.2 (0.940)	45 ± 14.1 (0.985)	89 ± 8.5 (0.991)	1.4 ± 0.6 (0.993)	1.8 ± 0.4 (0.998)	1.9 ± 0.1 (0.983)	6.8 ± 2.1 (0.719)	17 ± 2.1 (0.861)	22 ± 3.5 (0.681)

higher (Liang et al., 2013) values of rate constants than those reported in the literature for other plant proteins. These discrepancies are primarily due to differences in the experimental setup, e.g., equilibration time, type of oils and proteins, the instrumental setup etc. As these rate constants are not a material property, they can be comfortably used to determine and directly compare the kinetic behaviour of proteins within a specific experimental setup. The kinetic analysis generally showed modest differences between the proteins irrespective of their compositional differences. Inspection of the kinetic parameters of all interfaces shows that kinetic processes are generally faster at the oil surfaces and follow the order (slower) air < triglyceride < terpene (faster). This may be due to the improved solubility of proteins in terpene that facilitates exposure of the hydrophobic amino acids and protein unfolding. It is noteworthy to mention that extraction conditions (e.g., temperature and pH of extraction, drying conditions etc.) influence protein structure (i.e., native vs denatured), which is generally a determinant factor of their functionality. For instance, globular protein denaturation results in unfolding, and it has been shown that at interfaces, globular proteins behave differently than flexible (Erni, Windhab, & Fischer, 2011). Surface hydrophobicity relates to the number of hydrophobic amino acids at the protein's surface. Early works, carried out primarily with animal protein sources, have linked surface hydrophobicity to the protein's ability to reduce surface tension (Nakai, 1983). In recent literature focusing on plant proteins, more complex relationships emerge with no clear link between surface hydrophobicity and surface or interfacial tension reduction. For instance, literature is abundant with research on legume (Ge et al., 2021; Johnston, Nickerson, & Low, 2015; Karaca, Low, & Nickerson, 2011b; Singhal, Stone, Vandenberg, Tyler, & Nickerson, 2016) and non-legume proteins (Cheung, Wanasundara, & Nickerson, 2015; Karaca, Low, & Nickerson, 2011a) that do not find and a direct relationship, indicating that energy barriers to adsorption or other factors may come into play. Indeed, recent fundamental work revealed that protein adsorption dynamics not only depend on the protein folding, molecular size, and distribution of hydrophobic residues along the protein but also the oil polarity. Additionally, proteins present different behaviour at the air-water surface than at the oil-water interfaces due to the absence of hydrophobic interactions with the subphase (Bergfreund et al., 2021). The present work also highlights that the details of isolate preparation are irrelevant to the interfacial adsorption kinetics, as no striking differences have been observed, particularly between the legume protein isolates. It is possible that in such complex protein mixtures, the chemical composition of the subphase and protein conformational rearrangements are the main factors affecting adsorption kinetics.

Although kinetic analysis of protein diffusion gives first insights into protein behaviour, it is not a reliable indicator of functionality at the interfaces. Consequently, we proceeded to quantify the rigidity of their interfacial films that provide a deeper understanding of their functional properties, which is discussed in the next section.

3.3. Dilatational rheology

On arrival at the interface, the exposed amino acids interact intermolecularly with adjacent protein chains leading to the formation of a viscoelastic film (Murray, 2002). Consequently, interfacial protein layers are no longer characterised by their ability to lower the interfacial tension but by the film's viscoelasticity (Sagis & Fischer, 2014a). To investigate the mechanical properties of the interfacial films, dilatational rheology was employed for the systems with a nominal concentration of 1 mg/mL.

Generally, at the air surface, proteins tend to form more elastic films than at the oil interfaces, with the dilatational storage modulus (E') reaching values > 35 mN/m (Fig. 4 a-c). The least elastic films were formed at the myrcene interfaces for all protein isolates investigated

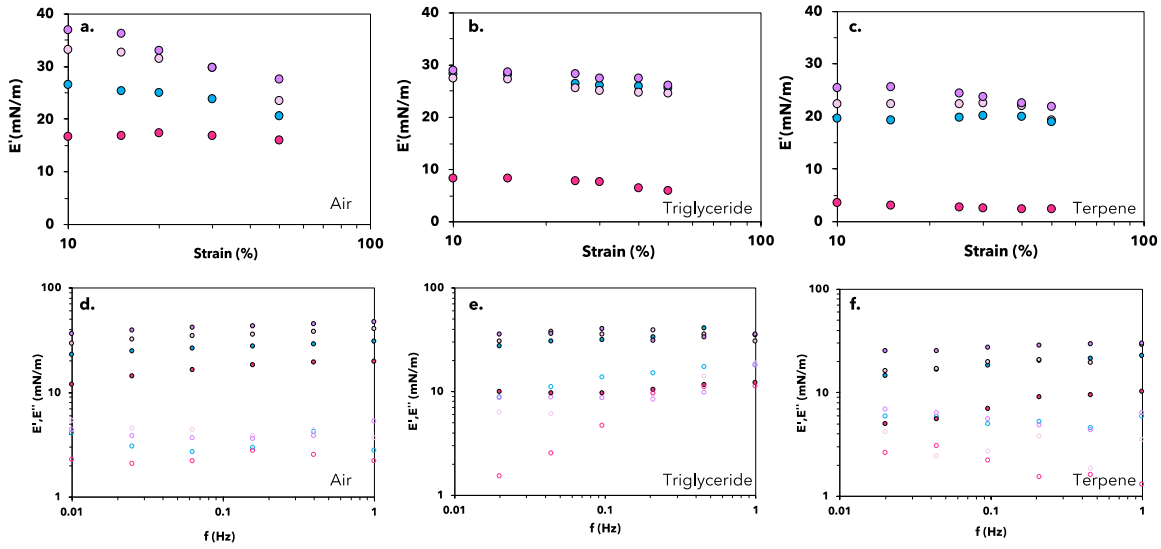

Fig. 4. Oscillatory measurements of protein isolates interfaces stabilised by PP (●), SP (○), RP (●) and MBP (●) at 1 mg/mL. **Top**: Amplitude sweeps of systems at the a) air, b) triglyceride, and c) terpene interfaces (frequency, 0.1 Hz). **Bottom**: Mechanical spectra of systems at the d) air, e) triglyceride, and f) terpene interfaces ($\Delta A/A_o$ 10%). Filled markers represent the elastic dilatational (E′) and open markers the loss dilatational (E″) moduli.

(<25 mN/m). The strain dependence was generally greater for the air than oil interfaces indicating that proteins exhibit weaker lateral interactions in agreement with previously published work (Hinderink, Sagis, Schroën, & Berton-Carabin, 2020). Consequently, films formed at oil interfaces are less rigid and can withstand higher strains. For instance, in protein-stabilised interfaces able to form very strong lateral interactions, E′ declines rapidly with amplitude (Hinderink et al., 2020; Mitropoulos et al., 2014; Xia et al., 2022). Weaker interactions at the oil interfaces are easily rationalised as hydrophobic amino acids have a greater affinity for the oil, thus weakening the inter-amino acid interactions.

Investigation of films' viscoelastic properties as a function of time can be achieved by constructing the mechanical spectra of the surfaces (Fig. 4 d-f). All systems exhibited negligible frequency dependence, with the E' dominating the viscous dilatational modulus ($E´´$) throughout the experimental window. Little frequency dependence is indicative of well-structured interfacial films as the imposed changes in the surface area ($\Delta A/A_o$) do not influence relaxation processes in either short (high frequency, fast relaxation times) or long (low frequency, slow relaxation times) timescales. When the interface is deformed in dilatational measurements, the rheological response is usually due to the deformed microstructure and friction with the subphase. Alternatively, the observed rheological responses may result from other transport phenomena, e.g., mass transfer, relaxation processes in the surface layer or diffusional exchanges with the bulk solution (Felix, Yang, Guerrero, & Sagis, 2019; Fuller & Vermant, 2012; Möbius & Miller, 1998).

The ionic strength of the buffer and the dielectric constant of the oils are two key factors that may also affect the strength of protein interactions. The higher dielectric constant of MCT (3.9) compared to that of myrcene (2.3) and the presence of salt (100 mM NaCl) shorten the repulsion range between proteins strengthening the attractive interactions leading to films with a higher elasticity (Fig. 4). Legume proteins showed similar behaviour, particularly at the oil interfaces, demonstrating that protein compositional characteristics (Table 1, Fig. 1) do not play a major role in influencing interactions between protein chains, in agreement with the kinetic modelling presented above. Rice protein exhibited lower elasticities, indicating a less resilient structure and weaker lateral protein interactions. Our results are in agreement with dynamic data from other plant protein systems under similar environmental conditions (Felix, Romero, Carrera-Sanchez, & Guerrero, 2019; Rodríguez Patino, Molina Ortiz, Carrera Sánchez, Rodríguez Niño, & Añón, 2003; Romero et al., 2012; Tamm, Herbst, Brodkorb, & Drusch, 2016). In conclusion, the overall change in the strength of elasticity occurs because the strength of hydrophobic interactions between amino acids is reduced at the oil interfaces because of the solvation, leading to weaker interfacial films (Bergfreund et al., 2018; Graham & Phillips, 1979c; Wüstneck, Moser, & Muschiolik, 1999).

Plots of π vs $\Delta A/A_o$ outside the LVR, known as Lissajous plots, provide additional information on the behaviour of the interfaces on extension and compression (Fig. 5). The construction of Lissajous plots allows the inclusion of non-linear effects into the analysis in contrast to measurements only within the LVR. Briefly, a linear viscoelastic response of the interface results in an elliptical Lissajous plot. Deviations from linearity result in asymmetries revealing how the interface behaves in compression and extension (Sagis & Scholten, 2014b).

At low deformation within the LVR (Fig. 5a), all systems displayed an elliptical Lissajous plot, a hallmark of a viscoelastic interface ($\Delta A/A_o =$ 10%). An increase of $\Delta A/A_o$ to 20% results in the onset of asymmetries, with their intensities varying depending on the protein and the subphase (Fig. 5b). Increasing deformation beyond 20% (Fig. 5 c and d), all systems studied exhibited strain-hardening on compression and strain-softening behaviour on extension, typical of protein interfaces (Sagis et al., 2014a). This indicates that the interfacial network is disrupted as it stretches on extension. In compression, the surfaces have a greater tendency to approach a jammed state as the surface density of protein clusters and interactions between them increase (Sagis et al., 2014a; Yang, de Wit, et al., 2022).

Constructing Lissajous plots at $\Delta A/A_o$ of 30% for all systems reveals clear differences between the mechanical properties of the interfaces, something that was not visible with measurements only within the LVR. At the air interfaces, the strain-hardening behaviour of protein films upon compression followed the order (stronger) MBP > SP > PP > RP (weaker) (Fig. 6a). At triglyceride interfaces, the asymmetries became less prominent, and the ellipses narrowed, indicating a predominantly elastic interfacial film (Fig. 6b). For the rice proteins, the curve is mostly linear, with a very low ability of the droplet to follow the imposed deformation. Such behaviour, previously observed in plant-dairy protein blends at oil-water interfaces (Hinderink et al., 2020), indicates that protein surface concentration increases when the surface is compressed

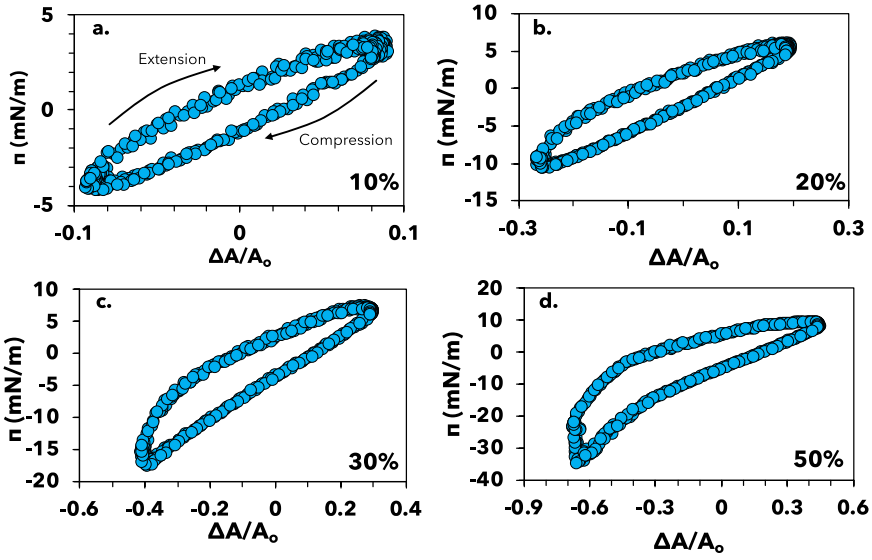

Fig. 5. Typical Lissajous plots, in the a) linear viscoelastic (10%), and non-linear viscoelastic interfaces at deformations of b) 20%, c) 30%, and d) 50%. Plots shown are for the MBP at the air surface.

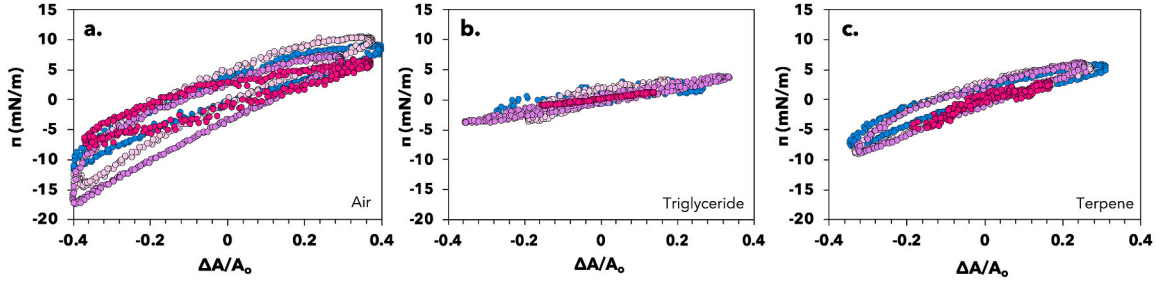

Fig. 6. Lissajous plots of protein isolates at 1 mg/mL and $\Delta A/A_o$ of 30% (0.1 Hz) at the a) air, b) triglyceride and c) terpene interfaces. PP (●), SP (○), RP (●) and MBP (●).

and decreases when it is extended. A similar Lissajous plot shape was also observed at the terpene interfaces but with more evident asymmetries (Fig. 6c).

4. Conclusions

The interfacial behaviour of four plant protein concentres (pea, soy, mung bean, rice) was investigated at three interfaces (air, triglyceride, terpene) employing kinetic modelling of adsorption and dilatational rheology at pH 7.0 in the presence of salt. While proteins differed substantially in their composition, their interfacial behaviour was mainly dependent on the properties of the subphase. The end of the induction period for adsorption was between 10 and 100 s, regardless of the interface and protein. All proteins diffuse faster towards the terpene interface. Once at the interface, protein rearrangements at the triglyceride were twice as fast as those at the air interfaces (k_{rear} ~7 *vs* 14 × 10^{-3} s^{-1}) whereas configurational rearrangements at the terpene interfaces were the fastest (k_{rear} ~21 × 10^{-3} s^{-1}). Inspection of the kinetic parameters of all interfaces shows that kinetic processes are generally faster at the oil surfaces and follow the order (slower) air < triglyceride < terpene (faster). Proteins tend to form more elastic films at the air surface than at the oil interfaces, with the E′ reaching values > 35 mN/m. The least elastic films were formed at the myrcene interfaces for all protein isolates investigated (E′ < 25 mN/m). The chemical characteristics of the subphase play a determinant role in the elasticity of plant protein concentrates and follow the order (higher) air > triglyceride > terpene (lower).

Overall, the results show that tailoring the chemical characteristics of the oil phase should be of primary concern when structuring multiphasic systems with plant proteins. Additionally, the legume proteins showed similar interfacial performance, while rice proteins had the poorest functionality in all systems studied.

Author statement

Vassilis Kontogiorgos: Investigation, Data Curation, Formal Analysis, Writing - Original Draft, Conceptualization, Methodology, Writing - Review & Editing, Supervision, Project administration. **Sangeeta Prakash**: Writing - Review & Editing, Resources.

Declaration of competing interest

The authors declare that they have no known competing financial interests or personal relationships that could have appeared to influence the work reported in this paper.

Data availability

The data that has been used is confidential.

References

Aiking, H., & de Boer, J. (2020). The next protein transition. *Trends in Food Science & Technology, 105*, 515–522.

Bergfreund, J., Bertsch, P., & Fischer, P. (2021). Adsorption of proteins to fluid interfaces: Role of the hydrophobic subphase. *Journal of Colloid and Interface Science, 584*, 411–417.
Bergfreund, J., Bertsch, P., Kuster, S., & Fischer, P. (2018). Effect of oil hydrophobicity on the adsorption and rheology of β-lactoglobulin at oil–water interfaces. *Langmuir, 34*(16), 4929–4936.
Beverung, C. J., Radke, C. J., & Blanch, H. W. (1999). Protein adsorption at the oil/water interface: Characterization of adsorption kinetics by dynamic interfacial tension measurements. *Biophysical Chemistry, 81*(1), 59–80.
Bos, A., Martin, & van Vliet, T. (2001). Interfacial rheological properties of adsorbed protein layers and surfactants: A review. *Advances in Colloid and Interface Science, 91*(3), 437–471.
Bradford, M. M. (1976). A rapid and sensitive method for the quantitation of microgram quantities of protein utilizing the principle of protein-dye binding. *Analytical Biochemistry, 72*(1), 248–254.
Chang, C., Tu, S., Ghosh, S., & Nickerson, M. T. (2015). Effect of pH on the inter-relationships between the physicochemical, interfacial and emulsifying properties for pea, soy, lentil and canola protein isolates. *Food Research International, 77*, 360–367.
Cheung, L., Wanasundara, J., & Nickerson, M. T. (2015). Effect of pH and NaCl on the emulsifying properties of a napin protein isolate. *Food Biophysics, 10*(1), 30–38.
Day, L. (2013). Proteins from land plants – potential resources for human nutrition and food security. *Trends in Food Science & Technology, 32*(1), 25–42.
Djoullah, A., Djemaoune, Y., Husson, F., & Saurel, R. (2015). Native-state pea albumin and globulin behavior upon transglutaminase treatment. *Process Biochemistry, 50*(8), 1284–1292.
Drusch, S., Klost, M., & Kieserling, H. (2021). Current knowledge on the interfacial behaviour limits our understanding of plant protein functionality in emulsions. *Current Opinion in Colloid & Interface Science, 56*, Article 101503.
Ducel, V., Richard, J., Popineau, Y., & Boury, F. (2004). Adsorption kinetics and rheological interfacial properties of plant proteins at the Oil−Water interface. *Biomacromolecules, 5*(6), 2088–2093.
Eastoe, J., & Dalton, J. S. (2000). Dynamic surface tension and adsorption mechanisms of surfactants at the air–water interface. *Advances in Colloid and Interface Science, 85*(2), 103–144.
Erni, P., Windhab, E. J., & Fischer, P. (2011). Emulsion drops with complex interfaces: Globular versus flexible proteins. *Macromolecular Materials and Engineering, 296*(3–4), 249–262.
Felix, M., Romero, A., Carrera-Sanchez, C., & Guerrero, A. (2019). Assessment of interfacial viscoelastic properties of Faba bean (Vicia faba) protein-adsorbed O/W layers as a function of pH. *Food Hydrocolloids, 90*, 353–359.
Felix, M., Yang, J., Guerrero, A., & Sagis, L. M. C. (2019). Effect of cinnamaldehyde on interfacial rheological properties of proteins adsorbed at O/W interfaces. *Food Hydrocolloids, 97*, Article 105235.
Fuller, G. G., & Vermant, J. (2012). Complex fluid-fluid interfaces: Rheology and structure. *Annual Review of Chemical and Biomolecular Engineering, 3*(1), 519–543.
Ge, J., Sun, C.-X., Mata, A., Corke, H., Gan, R.-Y., & Fang, Y. (2021). Physicochemical and pH-dependent functional properties of proteins isolated from eight traditional Chinese beans. *Food Hydrocolloids, 112*, Article 106288.
Graham, D. E., & Phillips, M. C. (1979a). Proteins at liquid interfaces: I. Kinetics of adsorption and surface denaturation. *Journal of Colloid and Interface Science, 70*(3), 403–414.
Graham, D. E., & Phillips, M. C. (1979b). Proteins at liquid interfaces: II. Adsorption isotherms. *Journal of Colloid and Interface Science, 70*(3), 415–426.
Graham, D. E., & Phillips, M. C. (1979c). Proteins at liquid interfaces: III. Molecular structures of adsorbed films. *Journal of Colloid and Interface Science, 70*(3), 427–439.
Hinderink, E. B. A., Sagis, L., Schroën, K., & Berton-Carabin, C. C. (2020). Behavior of plant-dairy protein blends at air-water and oil-water interfaces. *Colloids and Surfaces B: Biointerfaces, 192*, Article 111015.
Johnston, S. P., Nickerson, M. T., & Low, N. H. (2015). The physicochemical properties of legume protein isolates and their ability to stabilize oil-in-water emulsions with and without genipin. *Journal of Food Science & Technology, 52*(7), 4135–4145.
Karaca, A. C., Low, N., & Nickerson, M. (2011a). Emulsifying properties of canola and flaxseed protein isolates produced by isoelectric precipitation and salt extraction. *Food Research International, 44*(9), 2991–2998.
Karaca, A. C., Low, N., & Nickerson, M. (2011b). Emulsifying properties of chickpea, faba bean, lentil and pea proteins produced by isoelectric precipitation and salt extraction. *Food Research International, 44*(9), 2742–2750.
Liang, H.-N., & Tang, C.-H. (2013). Emulsifying and interfacial properties of vicilins: Role of conformational flexibility at quaternary and/or tertiary levels. *Journal of Agricultural and Food Chemistry, 61*(46), 11140–11150.
Li, M., McClements, D. J., Liu, X., & Liu, F. (2020). Design principles of oil-in-water emulsions with functionalized interfaces: Mixed, multilayer, and covalent complex structures. *Comprehensive Reviews in Food Science and Food Safety, 19*(6), 3159–3190.
Liu, F., Chen, Z., & Tang, C.-H. (2014). Microencapsulation properties of protein isolates from three selected Phaseolus legumes in comparison with soy protein isolate. *LWT - Food Science and Technology, 55*(1), 74–82.
Loveday, S. M. (2019). Food proteins: Technological, nutritional, and sustainability attributes of traditional and emerging proteins. *Annual Review of Food Science and Technology, 10*(1), 311–339.
Ma, K. K., Greis, M., Lu, J., Nolden, A. A., McClements, D. J., & Kinchla, A. J. (2022). Functional performance of plant proteins. *Foods, 11*(4).
Mendoza, E. M. T., Adachi, M., Bernardo, A. E. N., & Utsumi, S. (2001). Mungbean [vigna radiata (L.) wilczek] globulins: Purification and characterization. *Journal of Agricultural and Food Chemistry, 49*(3), 1552–1558.
Mileti, O., Baldino, N., Carmona, J. A., Lupi, F. R., Muñoz, J., & Gabriele, D. (2022). Shear and dilatational rheological properties of vegetable proteins at the air/water interface. *Food Hydrocolloids, 126*, Article 107472.
Mitropoulos, V., Mütze, A., & Fischer, P. (2014). Mechanical properties of protein adsorption layers at the air/water and oil/water interface: A comparison in light of the thermodynamical stability of proteins. *Advances in Colloid and Interface Science, 206*, 195–206.
Möbius, D., & Miller, R. (1998). *Proteins at liquid interfaces*. Amsterdam New York: Elsevier.
Murray, B. S. (2002). Interfacial rheology of food emulsifiers and proteins. *Current Opinion in Colloid & Interface Science, 7*(5), 426–431.
Nakai, S. (1983). Structure-function relationships of food proteins: With an emphasis on the importance of protein hydrophobicity. *Journal of Agricultural and Food Chemistry, 31*(4), 676–683.
Nishinari, K., Fang, Y., Guo, S., & Phillips, G. O. (2014). Soy proteins: A review on composition, aggregation and emulsification. *Food Hydrocolloids, 39*, 301–318.
Poirier, A., Stocco, A., Kapel, R., In, M., Ramos, L., & Banc, A. (2021). Sunflower proteins at air–water and oil–water interfaces. *Langmuir, 37*(8), 2714–2727.
Rodríguez Patino, J. M., Molina Ortiz, S. E., Carrera Sánchez, C., Rodríguez Niño, M. R., & Añón, M. C. (2003). Dynamic properties of soy globulin adsorbed films at the air–water interface. *Journal of Colloid and Interface Science, 268*(1), 50–57.
Romero, A., Beaumal, V., David-Briand, E., Cordobes, F., Guerrero, A., & Anton, M. (2012). Interfacial and emulsifying behaviour of rice protein concentrate. *Food Hydrocolloids, 29*(1), 1–8.
Sagis, L. M. C., & Fischer, P. (2014a). Nonlinear rheology of complex fluid–fluid interfaces. *Current Opinion in Colloid & Interface Science, 19*(6), 520–529.
Sagis, L. M. C., & Scholten, E. (2014b). Complex interfaces in food: Structure and mechanical properties. *Trends in Food Science & Technology, 37*(1), 59–71.
Sagis, L. M. C., & Yang, J. (2022). Protein-stabilized interfaces in multiphase food: Comparing structure-function relations of plant-based and animal-based proteins. *Current Opinion in Food Science, 43*, 53–60.
Shen, L., & Tang, C.-H. (2014). Emulsifying properties of vicilins: Dependence on the protein type and concentration. *Food Hydrocolloids, 36*, 278–286.
Sim, S. Y., Srv, A., Chiang, J. H., & Henry, C. J. (2021). Plant proteins for future foods: A roadmap. *Foods, 10*(8).
Singhal, A., Stone, A. K., Vandenberg, A., Tyler, R., & Nickerson, M. T. (2016). Effect of genotype on the physicochemical and functional attributes of faba bean (Vicia faba L.) protein isolates. *Food Science and Biotechnology, 25*(6), 1513–1522.
Tamm, F., Herbst, S., Brodkorb, A., & Drusch, S. (2016). Functional properties of pea protein hydrolysates in emulsions and spray-dried microcapsules. *Food Hydrocolloids, 58*, 204–214.
Van Der Borght, A., Vandeputte, G. E., Derycke, V., Brijs, K., Daenen, G., & Delcour, J. A. (2006). Extractability and chromatographic separation of rice endosperm proteins. *Journal of Cereal Science, 44*(1), 68–74.
Wang, J.-M., Xia, N., Yang, X.-Q., Yin, S.-W., Qi, J.-R., He, X.-T., et al. (2012). Adsorption and dilatational rheology of heat-treated soy protein at the oil–water interface: Relationship to structural properties. *Journal of Agricultural and Food Chemistry, 60*(12), 3302–3310.
Ward, A. F. H., & Tordai, L. (1946). Time-dependence of boundary tensions of solutions I. The role of diffusion in time-effects. *The Journal of Chemical Physics, 14*(7), 453–461.
Wojciechowski, K. (2022). Surface tension of native and modified plant seed proteins. *Advances in Colloid and Interface Science, 302*, Article 102641.
Wouters, A. G. B., Fierens, E., Rombouts, I., Brijs, K., Blecker, C., & Delcour, J. A. (2017). Air-water interfacial properties of enzymatically hydrolyzed wheat gluten in the presence of sucrose. *Food Hydrocolloids, 73*, 284–294.
Wüstneck, R., Moser, B., & Muschiolik, G. (1999). Interfacial dilational behaviour of adsorbed β-lactoglobulin layers at the different fluid interfaces. *Colloids and Surfaces B: Biointerfaces, 15*(3), 263–273.
Xia, W., Botma, T. E., Sagis, L. M. C., & Yang, J. (2022). Selective proteolysis of β-conglycinin as a tool to increase air-water interface and foam stabilising properties of soy proteins. *Food Hydrocolloids, 130*, Article 107726.
Yang, Z., Dai, L., Sun, Q., McClements, D. J., & Xu, X. (2022). Effect of molecular weight on the interfacial and emulsifying characteristics of rice glutelin hydrolysates. *Food Hydrocolloids, 128*, Article 107560.
Yang, J., de Wit, A., Diedericks, C. F., Venema, P., van der Linden, E., & Sagis, L. M. C. (2022). Foaming and emulsifying properties of extensively and mildly extracted Bambara groundnut proteins: A comparison of legumin, vicilin and albumin protein. *Food Hydrocolloids, 123*, Article 107190.